



Bergische Universität Wuppertal

Fachbereich Mathematik und Naturwissenschaften

Institute of Mathematical Modelling, Analysis and
Computational Mathematics (IMACM)

Preprint BUW-IMACM 15/35

Poitr Putek

**Mitigation of the cogging torque and loss
minimization in a permanent magnet machine
using shape and topology optimization**

October 2015

<http://www.math.uni-wuppertal.de>

Mitigation of the cogging torque and loss minimization in a permanent magnet machine using shape and topology optimization

Piotr Putek

Bergische Universität Wuppertal, Chair of Applied Mathematics and Numerical Analysis, Germany
Ernst-Moritz-Arndt Universität Greifswald, Department: Institute for Mathematics and Computer Science, Germany

Purpose: The paper presents the topology optimization method to design the rotor and the tooth base in the stator of the permanent magnet (PM) excited machine with the improved high-speed features. The topological and shape sensitivity through the Multi-Level Set Method (MLSM) have been used to attain an innovative design of both the rotor and stator made of different materials.

Design/methodology/approach: This framework is based on the application of the topological and the shape derivative, obtained by incorporating the AVM into the multi-level set method for the magnetoquasistatic system. The representation of the shape and their evolution during the iterative optimization process are obtained by the multi-level set method.

Findings: To find the optimal configuration of a PM machine, the stator and rotor poles were simultaneously optimized by redistributing the iron and the magnet material over the design domains. In this way, it was possible to obtain an innovative design which allows to reduce mechanical vibration and the acoustic noise caused by the Cogging Torque, while taking the back-EMF into account.

Originality/value: The novelty of the proposed method is to apply the modified multi-level-set algorithm with the Total Variation (TV) to the magnetoquasistatic optimization problem. Given the eddy currents phenomenon in the model of a PM machine, it was possible not only to optimize the structure of a PM machine but also to analyse electromagnetic losses distribution.

Keywords: Permanent magnet machine, Cogging torque, Back-EMF, Shape and topology optimization, Electromagnetic losses,

1. Introduction

Permanent magnet (PM) synchronous machines with the advantages of the high torque per mass, high power per unit volume and a relatively simple structure have become more popular nowadays, see, e.g., (Husain, 2005; Hughes, 2006; Gieras and Wing, 2008; Paplicki, 2010). In particular, this did result in its broad use in the automotive industry due to their high performance, efficiency, and power density, which are important requirements in the commercialized hybrid vehicle with a different hybridization level, e.g., (Makini *et al.*, 2008; May *et al.*, 2011; Putek *et al.*, 2014, Paplicki, 2014). The machine, however, is characterized by an inherently high level of the torque ripple (TR) that results in the mechanical vibration, acoustic noise, and some problems with the position or speed control in the application of drive systems. From this point of view, the effective design procedure is desired for the high-performance low torque applications, especially suitable for electric vehicles. Therefore, in such a type of an electric machine, designers aim to minimize the cogging torque (CT), while taking the harmonic contents in the back electromotive force (the back-EMF) into account. Both analyzed quantities together with the saturation of the magnetic circuits and converter related issues (Bianchi *et al.*, 2002) are well-known sources of the TR in the developed electromagnetic torque. A lot of research related to the minimization of the CR and TR, including the back-EMF analysis, have been reported in the literature, for example, (Li and Slemmon, 1988; Favre *et al.*, 1993; Zhu and Howe, 2000). Among them, the adjustment of the magnet arc width in regards to the slot pitch, the shifting of the pole pair, employing the fractional number of slots per pole and the skewing of either the stator or the rotor magnets belong to the most common methods for the reduction of the CT. The skewing of stator slots or rotor magnets can be also applied for the reduction of the amount of higher back EMF harmonics (Bianchi *et al.*, 2002). Other proposed solutions include employing dummy slots or dummy teeth in the stator laminations, and the shaping of the magnets. However, it is a problematic task to design a PM machine by taking into account either the description of the machine structure with a few geometrical parameters only (Di Barba *et al.*, 2012) or the distribution of one material separately in the rotor poles (Lim *et al.*, 2012) or considering only the stator (Lee *et al.*, 2003).

Therefore, this work deals with designing a PM machine – since the machine topology itself is a major contributor to the CT and the TR. As the shapes of the rotor poles and the tooth stator primarily determine the torque characteristics, this work focuses on the simultaneous optimization of the iron and magnet rotor poles as well as the stator tooth in the Electrically Controlled Permanent Magnet Excited Synchronous Machine (ECPSM)¹. Due to its particular construction, this machine allows to achieve the extended field-weakening capability and thus, it might be a suitable solution for automotive industry as a drive for electrical vehicles, for example. Therefore, in this work the optimal rotor poles and the tooth stator shape of the ECPSM for the minimum of CT and TR have been found by redistributing simultaneously the iron and magnet material over a design domain under consideration.

The new aspect of our work is to extend the application of the coupled multi-level and the topological gradient-based algorithm with the Total Variation technique (TV), proposed by (Putek *et al.*, 2014a; Putek *et al.*, 2014b), into the magnetoquasistatic optimization problem. Additionally, in contrast to our previous work, the Gâteaux derivative has been used to calculate the gradient of a multi-objective cost functional. Thus, this work focuses on the topology optimization of the ECPSM structure using a more realistic but still 2-D model,

¹ The investigation on the development of the ECPSM construction was conducted in the frame of the project called “The Electrically Controlled Permanent Magnet Excited Synchronous Machine (ECPSM) with application to electro-mobiles”, supported by the Polish Government under the Grant No. N510 508040.

where also the eddy current phenomena have been taken into account. Specifically, an analysis of the steady state eddy current problem in the time-harmonic regime has been carried out.

Table 1. Main design data of the ECPS machine

$2p$: number of poles	12
r_{ostat} : outer radius of the stator	67.5 mm
r_{istat} : inner radius of the stator	41.25 mm
l_{as} : axial length of the one part of the stator	35.0 mm
w_{oslot} : width of the slot opening	4.0 mm
ns : number of slots	36
m : number of phases	3
t_m : thickness of magnets (NdFeB, $B_r=1.2$ T)	3.0 mm

In this way, it was possible to optimize and analyze the ECPS machine with respect to not only mechanical vibration and the acoustic noise caused by the CT and the TR, but also the electromagnetic losses could be considered.

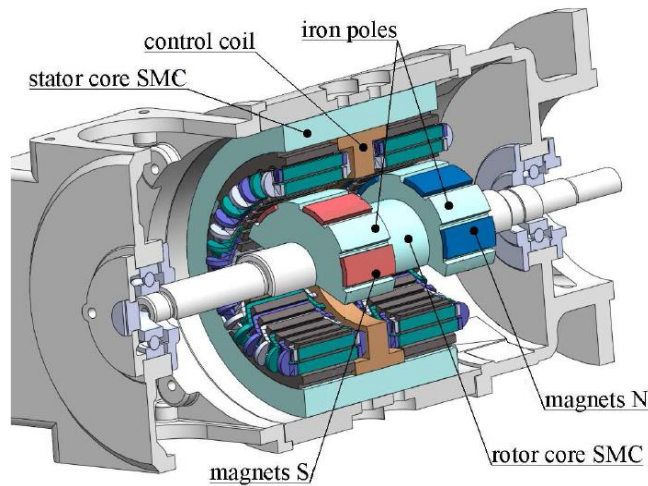


Figure 1. Cross-section of the ECPSM with the surface-mounted PM rotor and the stator structure (Pałka *et al.*, 2013)

2. Model description

A special construction, the so-called Electrically Controlled Permanent Magnet Excited Synchronous Machine, first proposed by May *et al.* (2011), has been analyzed in our work as a case study. The configuration of the ECPSM has been schematically depicted in Figure 1, while its main parameters has been included in Table 1. The rotor of the machine is divided into two sections. Each section consists of the radially magnetized in different directions (south and north) partial surface-mounted PMs. The stator, in turn, comprises the laminated core, a stator yoke made of the Soft Magnetic Composites (SMC) and the three phase armature windings, which are allocated in stator slots. A key feature of the machine construction is an additional circumferential excitation coil that is fixed in the axial center of the machine, between the rotor pole structures. The appropriate supply of this auxiliary coil by the DC-chopper allows to control the excitation level of the machine. Thus, the demagnetizing/magnetizing effect of the DC field winding can be observed. Consequently, the

effective field excitation produces induced voltages in the armature winding between zero and the maximum value, which is only limited by the saturation of the iron core (May *et al.*, 2012). In this way, it is possible to achieve the field weakening capability of 1:4 or even 1:5. The latter, besides the high torque, power and efficiency, the low level of the noise and vibration, is a very important requirement in case of the electro-mobiles applications. Technical parameters of a PM machine under consideration can be found in (May *et al.* 2011).

In this work, a two-dimensional (2-D) Finite Element (FE) model is applied to simulate the ECPS machine by the time-harmonic, parabolic-elliptic equation on bounded Lipschitz domain $D = D_{\text{air}} \cup D_{\text{FE}} \cup D_{\text{PM}}$

$$\nabla \times \nu(\nabla \times \mathbf{A}(\vec{r}) - \mathbf{B}_r(\vec{r})) + j\omega\sigma\mathbf{A}(\vec{r}) = \mathbf{J}^e(\vec{r}), \quad \vec{r} \in D \subset \mathbb{R}^2, \quad (2.1)$$

equipped with the Dirichlet boundary condition Γ_D on ∂D . Here, $\mathbf{A} = (0 \ 0 \ A)^T : D \rightarrow \mathbb{C}$ and $\mathbf{B} = \nabla \times \mathbf{A}$, $\mathbf{B}_r : D \rightarrow \mathbb{C}^2$ are phasors of the magnetic vector potential (MVP) and the magnetic flux density, respectively. The latter is defined in the 2-D model as

$$\mathbf{B} = (\partial_y A, \ -\partial_x A, \ 0)^T := \nabla \times (0, \ 0, \ A)^T, \quad (2.2)$$

which implies $|\mathbf{B}| = |\nabla A|$ with $|\cdot|$ the $L^2(D)$ -norm. The material properties σ and ν denote the conductivity and the reluctivity, more precisely $\nu = \nu_0 \cdot \nu_r$ with $\nu_r = (I, \ \nu_{\text{PM}}, \ \nu_{\text{FE}})$ stands for the relative reluctivity of free space, the permanent-magnet and soft iron, while ν_0 is the permeability of vacuum. \mathbf{B}_r denotes the remanent flux density of a PM, while $\mathbf{J}^e \in L^2(D)$, $\mathbf{J}^e = (0 \ 0 \ J)^T : D \rightarrow \mathbb{C}$ with the angular frequency ω refers to the forced current density in three phase single tooth windings. We also take the eddy currents phenomena in the PM and the iron parts into account in our 2-D model. However, the anisotropy and hysteresis effects have been disregarded. Furthermore, to reduce the computational burden, we use both the rotational symmetry utilizing the periodic boundary condition Γ_{PBC} (Nakata *et al.*, 1988) and the arbitrary Lagrangian-Eulerian method (Braess and Wriggers, 2000) for the simulation of the electric machine rotation.

2.1. Analysis of electromagnetic torque fluctuation

In general, the origin of the torque fluctuation is due to the highly non-linear and discrete nature of the torque production, which is mainly responsible for producing the TR and the CT and as a result, the speed variations (Chen *et al.*, 2002). Specifically, with reference to the sinusoidal PM machine with surface mounted magnets, there are primarily two contributions to the torque pulsation.

The electromagnetic torque T can be defined using the co-energy variation (Gieras and Wing, 2008) in the following way

$$T = \left. \frac{\partial W_{co}}{\partial \mathcal{G}} \right|_{i=const.} \quad (2.3)$$

However, in the case of the synchronous machine with surface mounted permanent magnets, both self and mutual inductance coefficients of the armature windings are independent of the rotor angular position \mathcal{G} (Borghi *et al.*, 1999). Therefore, the electromagnetic torque can be further expressed by

$$T = -\sum_{k=1}^{nr} \frac{e_k i_k}{\omega_m} + \frac{1}{2} \wp_m \frac{\partial P_m}{\partial \mathcal{G}}, \quad (2.4)$$

where nr means the number of phases, ω_m is a rotor angular speed and i_k is the stator winding current, \wp_m and P_m represent the equivalent magnetomotive force and the magnetic circuit permeance of the magnets, respectively. Furthermore, the back-EMF of the stator winding e_k is described by the time derivative of the flux-linkage Φ as follows

$$e_k = -j\omega\Phi. \quad (2.5)$$

When the flux-linkage is sinusoidal with respect to the rotor (Lee *et al.*, 2003), the back-EMF of each winding takes the sinusoidal waveform. This fact has been taken into account in the formulation of the optimization problem. The equation (2.4) shows the main contributions into the electromagnetic torque pulsation. Thus, the TR due to the field harmonics of the magnets is included in the EMF harmonic component (Jahns and Soong, 1996). On the other hand, the second term of the equation (2.4) allows to take the CT contribution into account.

The cogging torque T can be calculated using the Maxwell stress tensor method (Gieras and Wing, 2008) for no-current armature in a FE model

$$T = \nu_0 \oint_S \left(\mathbf{r} \times (n \cdot \mathbf{B}) \mathbf{B} - \frac{|\mathbf{B}|^2}{2} n \right) dx, \quad (2.6)$$

where n is the outward unit normal vector of any closed integration surface in the air-gap surrounding the rotor, denoted by S . It can be noted that, even if a machine is designed to the CT compensation, it can still generate the TR due to the higher harmonics current (Lee *et al.*, 2003). In turn, if the back-EMF takes a sinusoidal form and, simultaneously, the PM variation is reduced, the constant power and torque are obtained. This fact has been taken into account, while defining a cost functional.

3. Multi-level set approach

The level set method was originally proposed by Osher and Sethian (1988) in order to trace interfaces between different phases of fluids flows. More recently, this concept has been further generalized by Vese and Chan (2002) on the segment model with more than two domains and thus, called the multi-level set method. According to this methodology, for the description of the ECPSM geometry, three level set functions have to be employed to express five different domains with three different materials, such as the iron pole D_2 , the PM pole D_3 , the air area D_4 , the base tooth of the rotor made of iron D_5 and the air-tooth opening D_6 . Thus, in case of rotor poles, these domains have been defined by

$$\begin{aligned} D_1 &= \{\vec{r} \in \Omega \mid \phi_1 > 0 \text{ and } \phi_2 < 0\}, & D_2 &= \{\vec{r} \in \Omega \mid \phi_1 < 0 \text{ and } \phi_2 > 0\}, \\ D_3 &= \{\vec{r} \in \Omega \mid \phi_1 < 0 \text{ and } \phi_2 < 0\}, & D_4 &= \{\vec{r} \in \Omega \mid \phi_1 > 0 \text{ and } \phi_2 > 0\}, \end{aligned} \quad (3.1)$$

where a signed distance function has taken the form

$$\phi_i(\vec{r}) = \begin{cases} \min(|\vec{r} - \vec{r}_i|) & \vec{r}_i \in D_i \setminus \partial D_i, \\ 0 & \vec{r}_i \in \partial D_i, \end{cases} \quad (3.2)$$

where \vec{r}_I denotes I -th node on the boundary. In such a situation, the material properties of each rotor poles region can be described by the following equations

$$\begin{aligned}
\nu_r(\phi_1, \phi_2) &= \nu_{r_1}H(\phi_1)H(\phi_2) + \nu_{r_2}H(\phi_1)(1-H(\phi_2)) + \\
&\quad + \nu_{r_3}(1-H(\phi_1))H(\phi_2) + \nu_{r_4}(1-H(\phi_1))(1-H(\phi_2)), \\
\sigma(\phi_1, \phi_2) &= \sigma_1H(\phi_1)H(\phi_2) + \sigma_2H(\phi_1)(1-H(\phi_2)) + \\
&\quad + \sigma_3(1-H(\phi_1))H(\phi_2) + \sigma_4(1-H(\phi_1))(1-H(\phi_2)), \\
\mathbf{B}_r(\phi_1, \phi_2) &= \mathbf{B}_{r_1}H(\phi_1)H(\phi_2) + \mathbf{B}_{r_2}H(\phi_1)(1-H(\phi_2)) + \\
&\quad + \mathbf{B}_{r_3}(1-H(\phi_1))H(\phi_2) + \mathbf{B}_{r_4}(1-H(\phi_1))(1-H(\phi_2)).
\end{aligned} \tag{3.3}$$

The function $H(x)$ stands for the Heaviside step function. However, in practical computations, to obtain numerical robustness, the application of a smeared-out version of the step Heaviside function, i.e.

$$H_\alpha(\phi) = \frac{\alpha}{\pi(\phi^2 + \alpha^2)} \tag{3.4}$$

with a parameter α influenced the approximation of the function around zero, is recommended by Osher and Sethian (1988). It results from the fact that both functions in a precise sense are limits of the C^∞ function given in Chan and Tai (2004). Consequently, the derivative of the Heaviside step function $H_\alpha(\phi)$, the so-called Dirac function, takes the form

$$\Lambda_\alpha(\phi) = \frac{1}{\pi} \tan^{-1} \left(\frac{\phi}{\alpha} \right) + \frac{1}{2}. \tag{3.5}$$

In the same way, the base of the tooth shape in the stator can be expressed by the signed distance function ϕ_3 and then,

$$D_5 = \{ \vec{r} \in \Omega \mid \phi_3 > 0 \}, \quad D_6 = \{ \vec{r} \in \Omega \mid \phi_3 < 0 \}. \tag{3.6}$$

The material properties of the tooth base domain, however, are specified by

$$\nu_r(\phi_3) = \nu_{r_5}H(\phi_3) + \nu_{r_6}(1-H(\phi_3)), \quad \sigma(\phi_3) = \sigma_5H(\phi_3) + \sigma_6(1-H(\phi_3)). \tag{3.7}$$

The multi-level set model together with the boundaries, which are implicitly embedded as the zero-level set of ϕ_i , is shown on Figures 2 and 3, respectively. Now, if we assume that the changes of the shape are determined by a velocity field \mathbf{V}_i , more precisely its normal component (Haug *et al.*, 1986; Sokołowski and Zolesio, 1992)

$$d_t \vec{r}(t) = \mathbf{V}_i(\vec{r}(t), t), \tag{3.8}$$

then, the evolution of the corresponding level-set function can be described by the Hamilton-Jacobi-type equation (Osher and Sethian, 1988; Sethian, 1999)

$$\partial_t \phi_i = -\nabla \phi_i(\vec{r}, t) d_t \vec{r} = -\mathbf{V}_i \cdot \mathbf{n}_i \nabla \phi_i(\vec{r}, t) = V_{n_i} |\nabla \phi_i|, \tag{3.9}$$

where $n_i := \nabla \phi_i / |\nabla \phi_i|$ and $\mathbf{V}_i := d_t \vec{r}$ is the speed of the zero-level set that corresponds to the defined cost functional. In our work, it is further described by a velocity field vector.

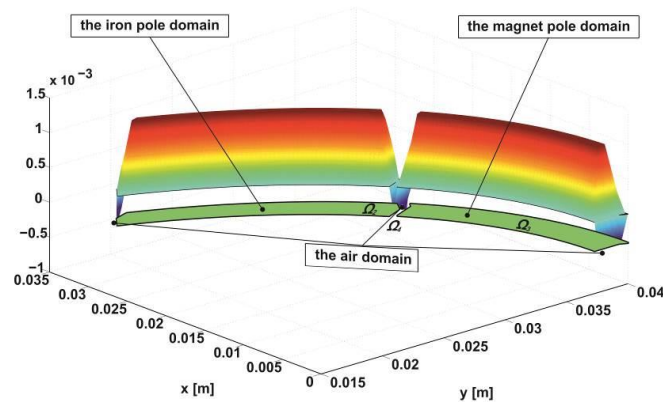


Figure 2. Signed distance functions with the zero level set of ϕ_1 and ϕ_2 for 2nd iteration of the optimization process

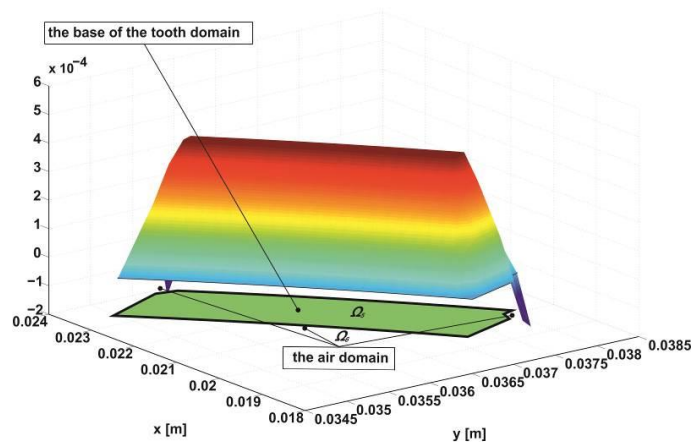


Figure 3. Signed distance function with the zero level set of ϕ_3 for 2nd iteration of the optimization process

Note that only the normal component of the velocity field contribute to the changes of a boundary, which is totally controlled by the zero level set function in this framework. In this work, the Adjoint Variable Method (AVM), see, e.g., (Durand *et al.*, 2009; Igarashi and Watanabe, 2010) has been used for the calculation of the speed of the zero-level set function.

4. Direct problem

Since the relativity has discontinuity across the boundary, we work with a weak formulation of the optimization problem.

4.1. Weak formulation

Let us define the parabolic-elliptic equation (2.1) for the magnetic vector potential in a weak formulation for the 2-D model

$$a(\varphi, A) = l_1(\varphi, \mathbf{B}_r) + l_2(\varphi, J) \quad (4.1)$$

with J being the external source different from zero and φ a suitable test function for A , $\varphi \in H^1(D)$. The symbol $H^1(D)$ denotes the Sobolev space of the complex-valued functions with first weak derivatives. Here, the sesquilinear and the linear load forms read as

$$a(\varphi, A) = (\nu \nabla \varphi, \nabla A)_D + j\omega(\sigma \varphi, A)_D = \int_D \nu \nabla \varphi \cdot \nabla A dx + j\omega \int_D \sigma \varphi \cdot A dx, \quad (4.2)$$

$$l_1(\varphi, \mathbf{B}_r) = (\nabla \varphi, \mathbf{B}_r)_D = \int_D \mathbf{B}_r \cdot \nabla \varphi dx, \quad (4.3)$$

$$l_2(\varphi, J) = (\varphi, J)_D = \int_D \varphi J dx, \quad (4.4)$$

with $(u, v)_{\Omega/\Gamma} = \int_{\Omega/\Gamma} u(\vec{r}) \cdot \overline{v(\vec{r})} dx$ the $L^2(D)^2$ inner product, where $\overline{u(\vec{r})}$ is the complex conjugate of $u(\vec{r})$. The induced norm has been defined as $\|u\| = \sqrt{(u, u)_{\Omega/\Gamma}}$.

4.2. Cost functional

Then, a cost functional for the multi-objective problem of the CT and/or the TR reduction in the 2-D magnetoquasistatic system, while taking the back-EMF as a second objective criterion, can finally be defined using the weighted aggregation method (Maler, 2009) as

$$\begin{aligned} F(\phi_1, \phi_2, \phi_3) &= w_1 T(\phi_1, \phi_2, \phi_3) + w_2 U(\phi_1, \phi_2, \phi_3) + \sum_{i=1}^3 \beta_i TV(\phi_i) \\ &= w_1 \frac{1}{2} r \cdot L_s \nu_0 \oint_l |\nabla A(\phi_1, \phi_2, \phi_3)|^2 dl \\ &\quad + w_2 \sum_{k=1}^{nr} \frac{L_s N \omega^2}{2S_k} \int_S |A(\phi_1, \phi_2, \phi_3)|^2 dx + \sum_{i=1}^3 \beta_i \int_D |\nabla \phi_i| dx, \end{aligned} \quad (4.5)$$

which is subjected to the following constraints

$$\begin{aligned} G_1(\phi_1, \phi_2) &= \int_D H(\phi_1)(1 - H(\phi_2)) dx / \int_D dx \leq S_{RFM}, \\ G_2(\phi_1, \phi_2) &= \int_D (1 - H(\phi_1))H(\phi_2) dx / \int_D dx \leq S_{RPM}, \\ G_3(\phi_3) &= \int_D H(\phi_3) dx / \int_D dx \leq S_{SFM}, \end{aligned} \quad (4.6)$$

Here, r is the radius of the circular path taken, L_s represents the axial length of the stator. In the equation (4.5), the $TV(\phi)$ denotes the total variation regularization (Vogel and Omam, 1998) with three coefficients such as β_1 , β_2 and β_3 introduced for controlling the complexity of the zero-level set functions. The parameter N refers to the number of winding turns, S is the cross-section area of windings, while nr represents the number of phases. It should be noticed that the proposed method requires *a priori* information about objective functions in the form of the assumed weight such that $w_1, w_2 > 0$ and $w_1 + w_2 = 1$. Therefore, the solution obtained in this way is not necessarily non-dominated (Putek *et al.*, 2012). The information about a more general methodology such as the Pareto front technique or the scalarizing multi-objective optimization method can be found, for example, in (Hawe and Sykulski, 2008; Di Barba, 2010). The prescribed coefficients S_{RFM} , S_{RPM} and S_{SFM} are specified as the area fraction of the PM and iron rotor parts as well as the area fraction of the base tooth in the stator, respectively.

5. Optimization problem

Since the multi-level set method has been used for the representation of both the rotor poles and the tooth base geometry, the optimal rotor design is defined as follows: find the distribution of the level set functions ϕ , for which a cost functional in the form of the equation (4.5), reaches its minimum considering the constraints expressed by the equation (4.6)

$$(\phi)_{\min} = \arg \min_{\phi_1, \phi_2, \phi_3 \in H^1(D)} F(\phi_1, \phi_2, \phi_3). \quad (5.1)$$

with $\phi = (\phi_1, \phi_2, \phi_3)$. In order to apply the gradient-based optimization method, first the Gâteaux derivative of F with respect to $p = (\nu, \sigma, \mathbf{B}_r, J)$ in a direction h has to be defined (Durand *et al.*, 2009)

$$\delta_h u = \delta_h u(p) = \lim_{\varepsilon \rightarrow 0} \frac{u(p + \varepsilon h) - u(p)}{\varepsilon} := \frac{du}{dp} h. \quad (5.2)$$

Then, the Gâteaux derivative of the first term, the so-called fidelity term $w_1 T[p(\phi)] + w_2 U[p(\phi)]$ of the cost functional defined by the equation (4.5) can be calculated as follows

$$\begin{aligned} \delta_\xi F &= w_1 r \cdot L_s \nu_0 \left[\left(\overline{\nabla \delta A(p)}, \nabla A(p) \right)_\Gamma + \left(\nabla \delta A(p), \overline{\nabla A(p)} \right)_\Gamma \right] \\ &+ w_2 \sum_{k=1}^{nr} \frac{L_s N \omega^2}{S_k} \left[\left(\overline{\delta A(p)}, A(p) \right)_D + \left(\delta A(p), \overline{A(p)} \right)_D \right] \\ &= w_1 r \cdot L_s \nu_0 2\Re \left[\left(\nabla \delta A(p), \nabla A(p) \right)_\Gamma \right] + w_2 \sum_{k=1}^{nr} \frac{L_s N \omega^2}{S_k} 2\Re \left[\left(\delta A(p), A(p) \right)_D \right] \end{aligned} \quad (5.3)$$

However, in the engineering problems, sometimes it is needed to calculate the total derivative with respect to an implicit function of a design vector variable p , for example, the CT $g(\nabla A(p))$ and the back-EMF $f(A(p))$. In such a situation, the approach proposed in (Dyck and Lowther, 1994; Kim *et al.*, 2004; Gawrylczyk and Putek, 2008) can be used without loss of the generality of the AVM application. As a result, in a dual problem, the following formula can be applied as a right side functional

$$\begin{aligned} \delta_\xi \tilde{F} &= w_1 \left[\left(\overline{\delta g(\nabla A(p))}, g(\nabla A(p)) \right)_\Gamma + \left(\delta g(\nabla A(p)), \overline{g(\nabla A(p))} \right)_\Gamma \right] \\ &+ w_2 \sum_{k=1}^{nr} \left[\left(\overline{\delta f_k(A(p))}, f_k(A(p)) \right)_D + \left(\delta f_k(A(p)), \overline{f_k(A(p))} \right)_D \right] \\ &= w_1 2\Re \left[\left(\lambda_\tau, g(\nabla A(p)) \right)_\Gamma \right] + w_2 \sum_{k=1}^{nr} 2\Re \left[\left(\lambda_\nu, f_k(A(p)) \right)_D \right]. \end{aligned} \quad (5.4)$$

where $\lambda_\tau = \partial_{\mathbf{B}} g$, $\lambda_\nu = \partial_A f$ are pseudo-source variables.

5.1. Sensitivity equation

For the purpose of the gradient calculation, the AVM has been used, see, e.g., (Park *et al.*, 1994; Park and Shin, 2003; Srinath and Mittal, 2010). This approach has been applied due to its lower computational burden in the comparison to such techniques as the differential

method or the sensitivity equation method. Hence, to calculate δF or $\delta \tilde{F}$ the knowledge of variations $\nabla \delta A(p)$ and $\delta A(p)$ is required. Therefore, according to the AVM, a weak formulation expressed by the equation (4.1) has been Gâteaux differentiated with respect to p in order to achieve the so-called sensitivity equation for desired quantities. For this purpose, first, one should consider the equation (4.1) for p and afterwards for $p + \varepsilon h$ as follows

$$\begin{aligned} (\nu \nabla \varphi, \nabla A(p))_D + j\omega(\sigma \varphi, A(p))_D &= (\nabla \varphi, \mathbf{B}_r(p))_D + (\varphi, J)_D, \\ ((\nu + \varepsilon \delta \nu) \nabla \varphi, \nabla A(p + \varepsilon \delta p))_D + j\omega((\sigma + \varepsilon \delta \sigma) \varphi, A(p + \varepsilon \delta p))_D &= \\ (\nabla \varphi, \mathbf{B}_r(p + \varepsilon \delta p))_D + (\varphi, J(p + \varepsilon \delta p))_D. \end{aligned}$$

Next, we apply the Gâteaux derivative for the resulted from subtracting both above equalities equation, which leads to

$$(\nu \nabla \varphi, \nabla \delta A)_D + j\omega(\sigma \varphi, \delta A)_D = -j\omega(\delta \sigma h \varphi, A)_D + (\nabla \varphi, \delta \mathbf{B}_r h)_D + (\varphi, \delta J h)_D. \quad (5.5)$$

Even though, we do not optimize the shape of winding slots in the stator but only the tooth base, we decided to leave the term related to J as a result of the applied form of a weak formulation. In this way, the same sesquilinear form $a(\varphi, \delta A)$ as in the equation (4.1) but with a different right side has been achieved. Furthermore, based on the Lax-Milgram theorem (Haug *et al.*, 1986), the existence and uniqueness of the solution of the sensitivity equation for δA can be proved. However, to avoid the calculation of δA from the equation for $h = 1, \dots, N$, resulted from the application of the FE analysis, we formulate the dual problem.

5.2. Dual problem

It has been demonstrated in the work (Conway 1997) that it is possible to define the dual problem using the linear operators \mathcal{Y} and \mathcal{Y}^* in such a way that

$$a(\varphi, u) = (\mathcal{Y}(\varphi), u)_D = (\varphi, \mathcal{Y}^*(u))_{D/\Gamma}. \quad (5.6)$$

Furthermore, taking the equation (5.6) into account, the dual problem for the sensitivity equation (5.6) with derivatives of a cost functional defined by equations (5.3) or (5.4) relies on finding $\zeta \in H^1(D)$, such that

$$a(\varphi, \zeta) = (\varphi, \mathcal{Y}^*(\zeta))_D = f(\varphi), \quad (5.7)$$

for all $\varphi \in H^1(\Omega)$, where the functional $f(\varphi)$ takes the form

$$f(\varphi) = \begin{cases} 2\Re \left[w_1 r \cdot L_s \nu_0 (\nabla \varphi, \nabla A)_\Gamma + w_2 \sum_{k=1}^{nr} L_s \frac{N \omega^2}{S_k} (\varphi, A)_D \right], & \text{for the equation (5.3)} \\ 2\Re \left[w_1 (\lambda_r, \varphi)_\Gamma + w_2 \sum_{k=1}^{nr} (\lambda_v, \varphi)_D \right], & \text{for the equation (5.4)} \end{cases} \quad (5.8)$$

Finally, the corresponding Gâteaux derivative of a cost functional can be written using the state variables and adjoint variables as follows

$$\delta F = 2\Re \left[-(\delta \nu \nabla \zeta, \nabla A) - j\omega(\delta \sigma \zeta, A) + (\nabla \zeta, \delta \mathbf{B}_r) + (\zeta, \delta J) \right]. \quad (5.9)$$

When the $A(p)$ has been calculated from the weak formulation defined by the equation (4.1) and $\zeta(p)$ from the dual problem, expressed by the equation (5.7), then the equation (5.9) allows to find the Gâteaux derivative of a cost functional in any direction.

5.3. Gradient of a cost functional

By the chain rule, it is easy to show, that following relation holds

$$\frac{\partial F}{\partial \phi_i} = \frac{\partial F}{\partial p_j} \frac{\partial p_j}{\partial \phi_i}, \quad i = 1, \dots, N_\phi, j = 1, \dots, N_p \quad (5.10)$$

where p_j is an element of the vector $p = (v_r, \sigma, \mathbf{B}_r, J)$ with the size N_p , $N_\phi = 3$. Finally, considering the piecewise constant functions represented by equations (3.3) and (3.6) as well as equations (5.9) and (5.10), it is possible to obtain

$$\frac{\partial F}{\partial \phi_1} = \frac{\partial F}{\partial p_j} (p_{j1} - p_{j3}) H_\alpha(\phi_2) \Lambda_\alpha(\phi_1) + \frac{\partial F}{\partial p_j} (p_{j2} - p_{j4}) (1 - H_\alpha(\phi_2)) \Lambda_\alpha(\phi_1), \quad (5.11)$$

$$\frac{\partial F}{\partial \phi_2} = \frac{\partial F}{\partial p_j} (p_{j1} - p_{j2}) H_\alpha(\phi_1) \Lambda_\alpha(\phi_2) + \frac{\partial F}{\partial p_j} (p_{j3} - p_{j4}) (1 - H_\alpha(\phi_1)) \Lambda_\alpha(\phi_2), \quad (5.12)$$

$$\frac{\partial F}{\partial \phi_3} = \frac{\partial F}{\partial p_j} (p_{j1} - p_{j2}) \Lambda_\alpha(\phi_3), \quad (5.13)$$

where $H_\alpha(\phi)$ and $\Lambda_\alpha(\phi)$ are the smeared-out version of the step Heaviside function and the Dirac function defined by equations (3.4) and (3.5).

5.4. Total variation regularization and constraints

In contrast to work by Yamada *et al.* (2010) and Lim *et al.* (2012), we incorporate the TV regularization technique into the multi-level set method in order to stabilize the optimization process and consequently, to indirectly control the length of the level sets. We were inspired by (Cimrák and Melicher, 2007), where the TV regularization was used to find the optimal shape design of a magnetic random access memory core using, however, a primal-dual approach. In our opinion, the penalization effect without smoothing edges might particularly be useful in case of the topology optimization of rotor poles and the tooth base made of nonlinear, ferromagnetic materials. It resulted from the fact that if the coefficient has large jumps, the use of the regularization in the sense of the $H^2(D)$ or $H^1(D)$ is not appropriate because of the discontinuities of the coefficient (Chan and Tai, 2004). Furthermore, for a non-differentiable function of coefficient q , $|\nabla q|$ can be understood strictly as a measure (Ziemer, 1989). It should be noted, however, that in our case the complexity of the structure, obtained by minimization a cost functional (4.5), can still be controlled by β_i coefficients. More precisely, in this work, we approximate the TV regularization functional by

$$TV(\phi) = \int_D |\nabla \phi| dx \approx \sum_i \sum_j \sqrt{|\phi_{i,j} - \phi_{i-1,j}|^2 + |\phi_{i,j} - \phi_{i,j-1}|^2} + \varepsilon \xi^2, \quad (5.14)$$

where, ξ means the order of the mesh size and ε is a positive constant by, for example, $\varepsilon \xi^2 = 10^{-10}$. Both parameters have been introduced in order to avoid dividing zero numbers for

the (i, j) rectangular element. In this way, ϕ is approximated by the piece constant value over mesh elements. Finally, the derivative of the regularization functional can be computed directly from (Chan and Tai, 2004, Putek *et al.*, 2014)

$$\frac{\partial R(\phi_i)}{\partial \phi_i} = \beta_i \nabla \cdot \left(\frac{\nabla \phi_i}{|\nabla \phi_i|} \right). \quad (5.15)$$

using either AVM (Vogel and Omam, 1998) or its numerical approximation of the filter defined by (5.14). In our work, we implemented the second approach.

Finally, the constraints defined by the equation (4.6) can naturally be involved in the scheme of the MLSM by using the Lagrange multiplier technique. Details of the derivation and implementation can be found in, e.g., (Osher and Santosa, 2001; Kim and Park, 2010; Yamada *et al.*, 2010; Lim *et al.*, 2012).

5.5. Topological Gradient approximation

Since the proper initialization of the multi-level-set-based algorithm could significantly accelerate the optimization process (Putek *et al.* 2014), the topological gradient (TG) method has been used for this purpose (Kim *et al.*, 2009; Putek *et al.*, 2012). Additionally, the application of both the shape and topological sensitivities results in a robust algorithm, which gives more flexibility in shape changing (Allaire *et al.* 2004; Burger *et al.*, 2004) and enables to escape local minima (He *et al.* 2007; Li and Lowther, 2011; Putek *et al.* 2014). Thus, by definition, the TG allows to measure the topology changes in the considered domain Ω and can be defined as (Schumacher *et al.*, 1996)

$$G(\vec{r}) = \lim_{d \rightarrow 0} \frac{F_o(\Omega \setminus B(\vec{r}, d)) - F_o(\Omega)}{\delta(\Omega)}, \quad (5.16)$$

with $\Omega \setminus B(\vec{r}, d) = \{ \vec{r} \in \Omega, |\vec{r}' - \vec{r}|_2 \geq d \}$, $\delta(\Omega) = -\text{area}(B(\vec{r}, d))$. Here, $F_o(\Omega)$ denotes a cost functional defined in domain Ω , while $B(\vec{r}, d)$ is the ball positioned at the point \vec{r} with the radius d . In case of the PDE with linear, isotropic materials, the problem is rather well studied, see, e.g., (Sokołowski and Zochowski 1999; Cea *et al.*, 2000; Amstutz *et al.*, 2007), including the topological expansion for the Maxwell equations by Masmoudi M. *et al.* (2005). Using this approach we achieve the formulas as in (Kim *et al.*, 2009; Putek *et al.*, 2012)

$$G_i(\vec{r}) = \begin{cases} 2 \cdot ((v_1 - v_2) \nabla A \cdot \nabla \zeta + j\omega(\sigma_1 - \sigma_2) A \cdot \zeta) & \text{in } D_2 \setminus B(\vec{r}, d), \\ 2 \cdot ((v_1 - v_3) \nabla A \cdot \nabla \zeta - (\mathbf{B}_{r1} - \mathbf{B}_{r3}) \cdot \nabla A + j\omega(\sigma_1 - \sigma_3) A \cdot \zeta) & \text{in } D_3 \setminus B(\vec{r}, d), \\ 2 \cdot ((v_5 - v_6) \nabla A \cdot \nabla \zeta + j\omega(\sigma_5 - \sigma_6) A \cdot \zeta) & \text{in } D_5 \setminus B(\vec{r}, d), \end{cases} \quad (5.17)$$

where ζ denotes the adjoint variable, which is the solution of the dual problem, defined by equation (5.7) with a right hand functional (5.4). Even though the topological gradient is defined in a different way than the derivative function with respect to the infinitesimal change of the material parameter, its computation does not require any additional computational burden.

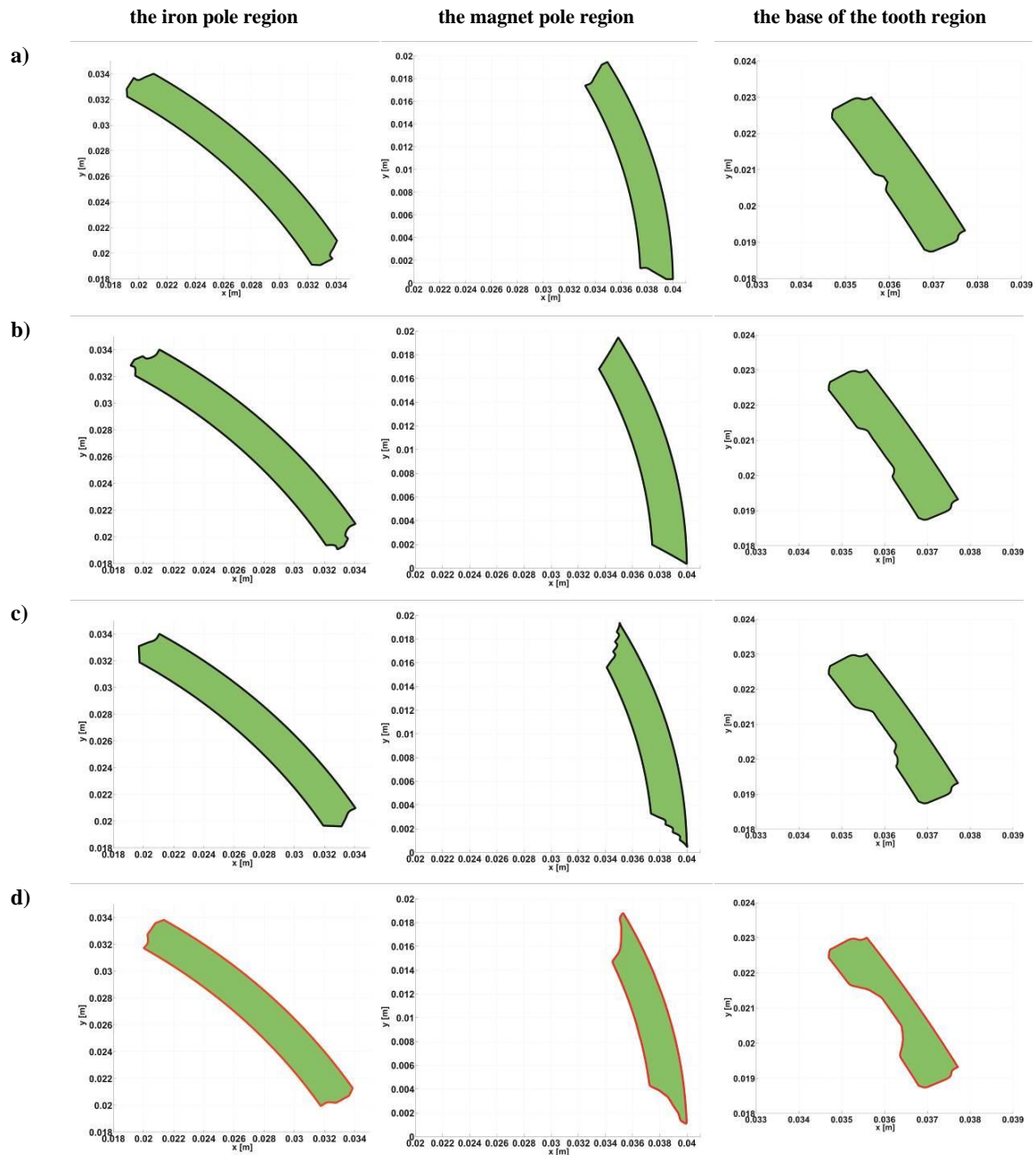


Figure 4. Evolution of the shapes of the one-pole pair and of the tooth base described by the zero-level set function in: a) 2th iteration, b) 5th iteration, c) 8th iteration and d) 13th iteration of the optimization process, where the last one presents the optimal solution.

6. Numerical results

The optimization procedure described in the previous section has now been further validated and applied to determine the optimal rotor poles and the base tooth shapes of the three phases, the six-pair of poles, the electrically controlled PM synchronous machine in case of no-load. The main parameters of the machine are given in Table 1. This solution enables to obtain the ultimate short machine designs in comparison with machines with drum type windings and allows to achieve the field weakening capability of 1:4 or even 1:5, what is a very important requirement in case of the electro-mobiles applications.

For the optimal topology design, shapes of the design domains after topological initialization in the first iteration is taken, as shown in Figure 2 and 3, respectively. In case of both, the rotor poles and the tooth base shape optimization, the evolution of the zero-level set function describing their shapes are shown in Figure 4. Furthermore, for the optimal configuration represented by the red line on the Figure 4, the numerical full 3D FE model in Flux3D has been built based on the result of the 2D optimization. The topology of both machines with the specification of their main parts before and after optimization is depicted on Figure 5.

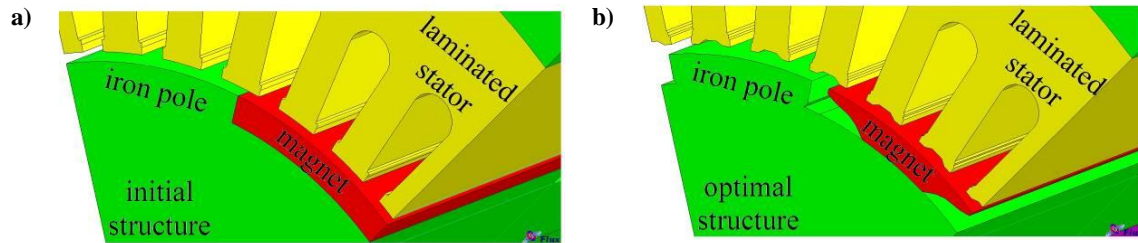


Figure 5. Comparison of the topology of the ECPSM for (a) initial and (b) optimal configuration.

Next, the mesh of 2D models and the magnetic field distribution in the initial and optimized structure under consideration is shown in Figure 6. Similarly, the 3D numerical models of one pair of pole of the ECPSM as well as the magnetic field distribution calculated for both structures are presented in Figure 7. For this purpose, a commercial software the Flux 3D (Flux 3D v.10.4.2, Cedrat, Meylan, 2013) has been used, while the algorithm for the 2D optimization has been implemented in the commercial software Comsol (COMSOL 3.5a, The COMSOL Inc., Burlington, MA, 2008) and Matlab (MATLAB 7.7, The MathWorks Inc., Natick, MA, 2008). The 3D FEA analysis of the CT for the initial and optimal structures has been conducted, shown on Figures 8a. The CT has been reduced averagely 91% for the optimized machine in comparison with the calculation performed in the initial structure.

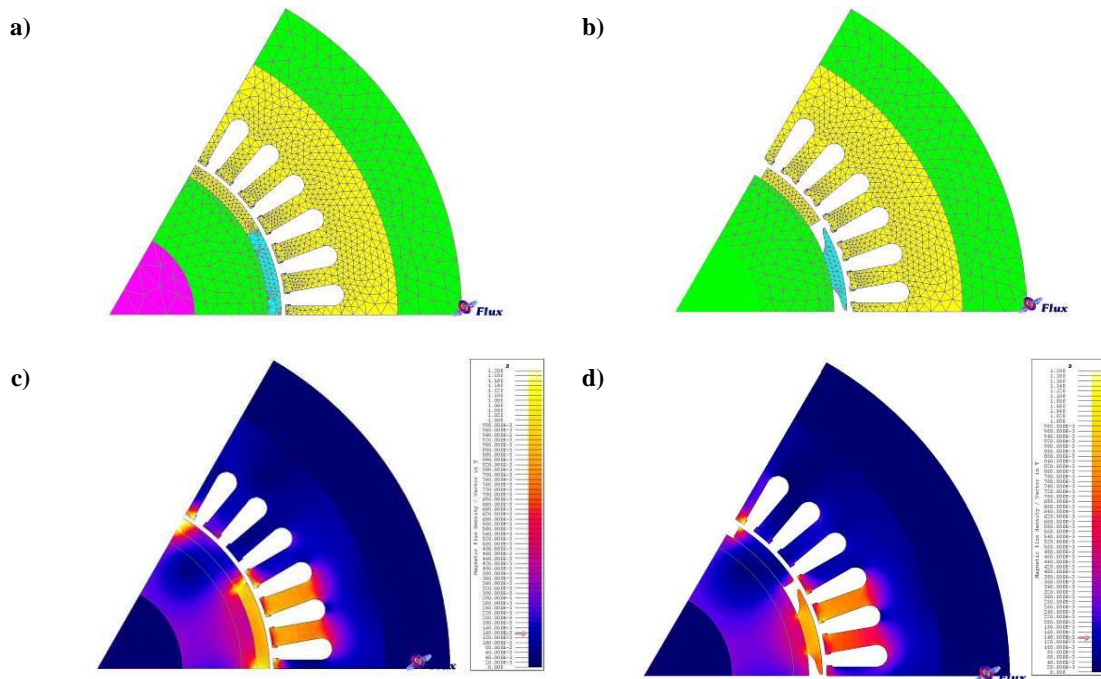


Figure 6. Mesh and magnetic field distribution in the initial model (a) and (c), as well as in the optimized 2D model (b) and (d).

model of one-pole pair of the ECPSM machine (b) and (d).

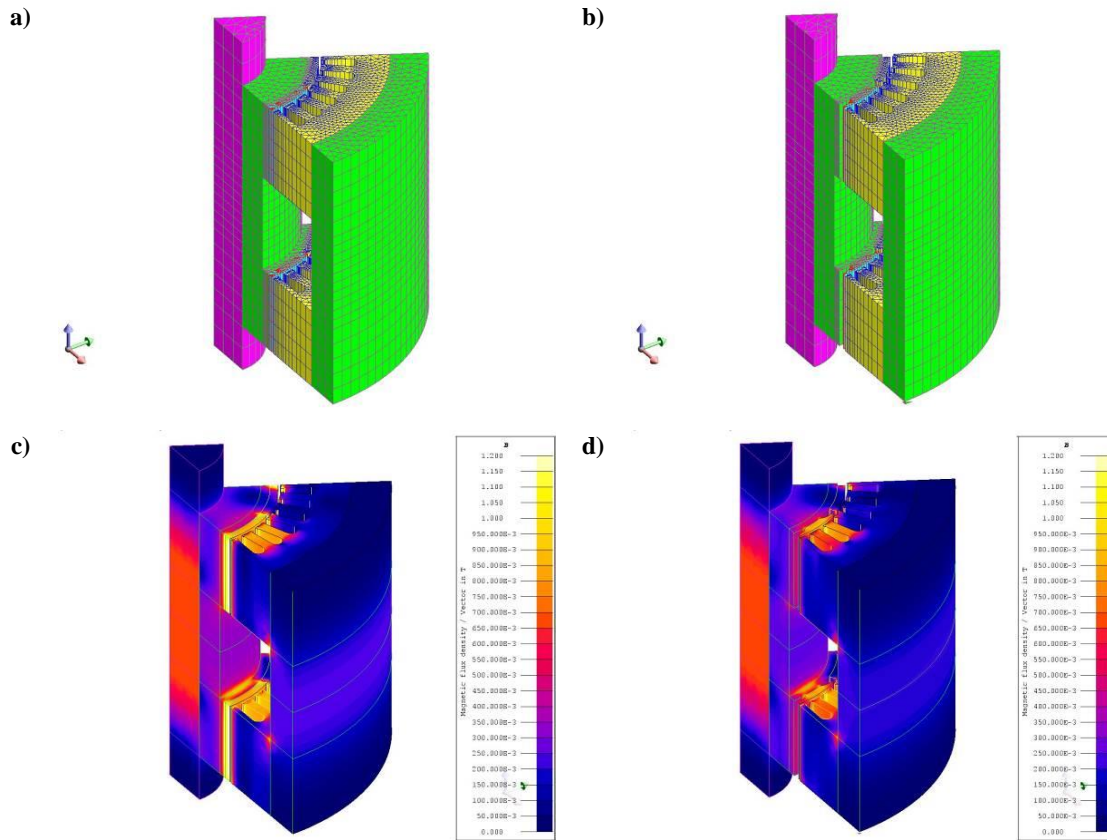
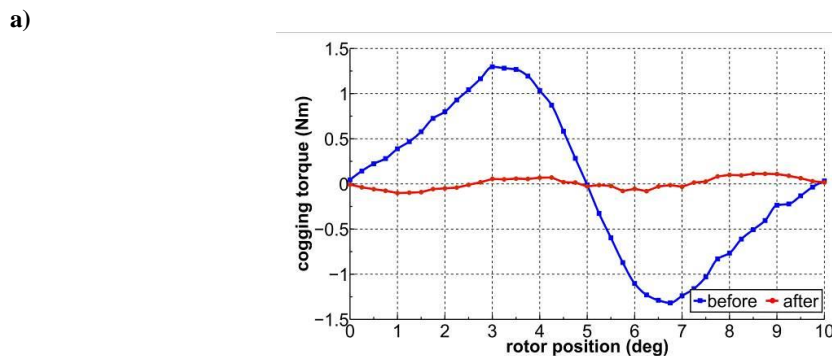
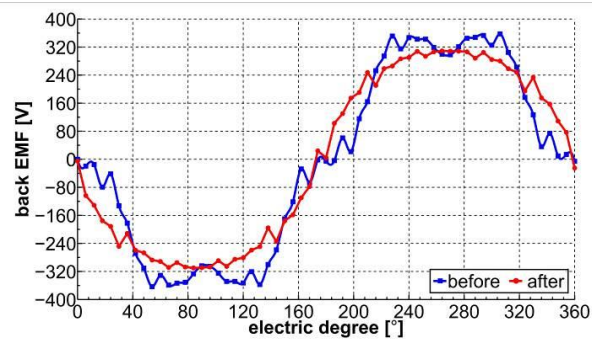


Figure 7. Mesh and magnetic field distribution in the initial model (a) and (c), as well as in the optimized 3D model of one-pole pair of the ECPSM machine (b) and (d).

Figures 8 b, in turn, presents the back-EMF waveform in the armature windings at 1000 rotor revolutions per minute (rpm) calculated for models before and after optimization. Moreover, the total harmonic distortion (THD) indicator including the fundamental plus harmonics as the reference shows approximately 63% reduction of higher harmonics of the back-EMF. However, the rectified mean values of EMF calculated for the optimized structure has dropped about 19%, while the magnetic flux density considered in the air-gap under magnet and iron poles has decreased around 16%. As a result, the rectified mean values of the electromagnetic torque shows about 18% decrease in comparison with the analogues quantity performed in the initial structure.



b)



c)

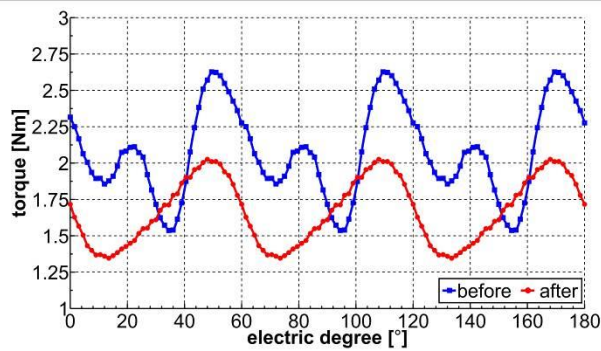


Figure 8. Analysis of the 3D FE model of the ECPSM machine before and after optimization: a) Cogging torque vs. rotor position calculated for both configurations, b) Back-EMF waveforms vs. electric degree at 1000 rpm, c) Electromagnetic torque vs electric degree for the initial and optimized structure with a sinusoidal armature current supply.

Moreover, even though during the optimization, the eddy currents losses have not been explicitly taken into account, an impact of the shapes of both the rotor poles and tooth base on the distribution of iron and magnet eddy currents has been investigated in the 3D FEA model before and after optimization.

Table 2. The coefficient values of Bertotti method for iron losses estimated in Flux3D

Considered quantities for sheet iron	Value	Unit
k_h : hysteresis loss coefficient	130.246	$[\text{WsT}^2/\text{m}^3]$,
σ : classical loss coefficient	1923077	$[\text{S/m}]$
k_e : loss in excess coefficient	0.357	$[\text{W}(\text{T/s})^{3/2}/\text{m}^3]$,
d : thickness of steel iron	$0.35 \cdot 10^{-3}$	$[\text{m}]$
k_f : fill factor	0.97	

For this purpose, the Bertotti method that has been implemented in Flux3D for iron losses and magnet eddy current losses has been used (Bertotti, 1988). Within the computation framework of Flux3D, the Bertotti losses has been defined as:

$$dP_{\text{moy}} = \left[k_h B_m^2 f + \frac{\pi^2 \sigma d^2}{6} (B_m f)^2 + k_e (B_m f)^{3/2} \cdot 8,67 \right] \cdot k_f \quad (5.18)$$

where k_h is the coefficient of losses by hysteresis, k_e is the coefficient of losses in excess, σ is the conductivity of the material (coefficient of classical eddy currents losses), d is the thickness of the lamination, k_f is the coefficient of filling that considers the electrical insulation of the laminations of the magnetic core (the stacking factor ($0 < k_f < 1$)), f frequency (except in Magneto Harmonic), B_m is the peak value of the magnetic flux density. In order to determine the k_e and k_h coefficients, the formula used in the Flux3D on a piece of material corresponding to 1 kg has been applied. The results of this estimation have been listed in Table 2.

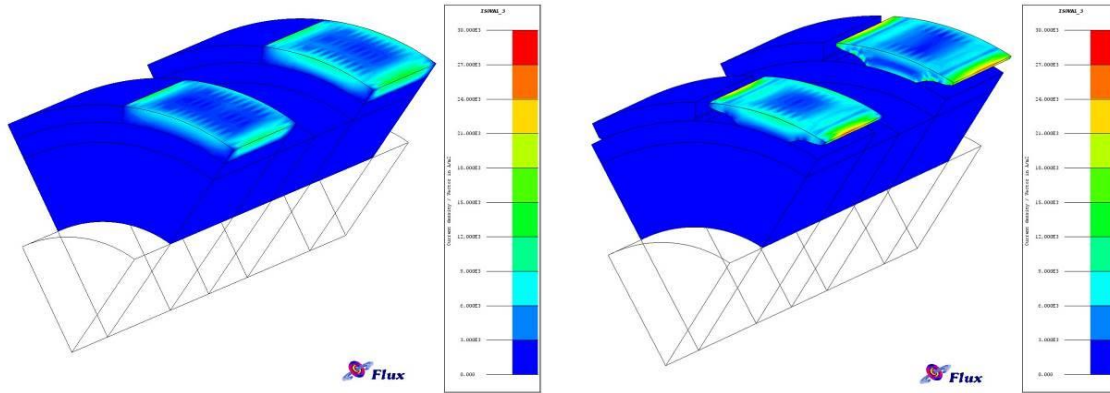
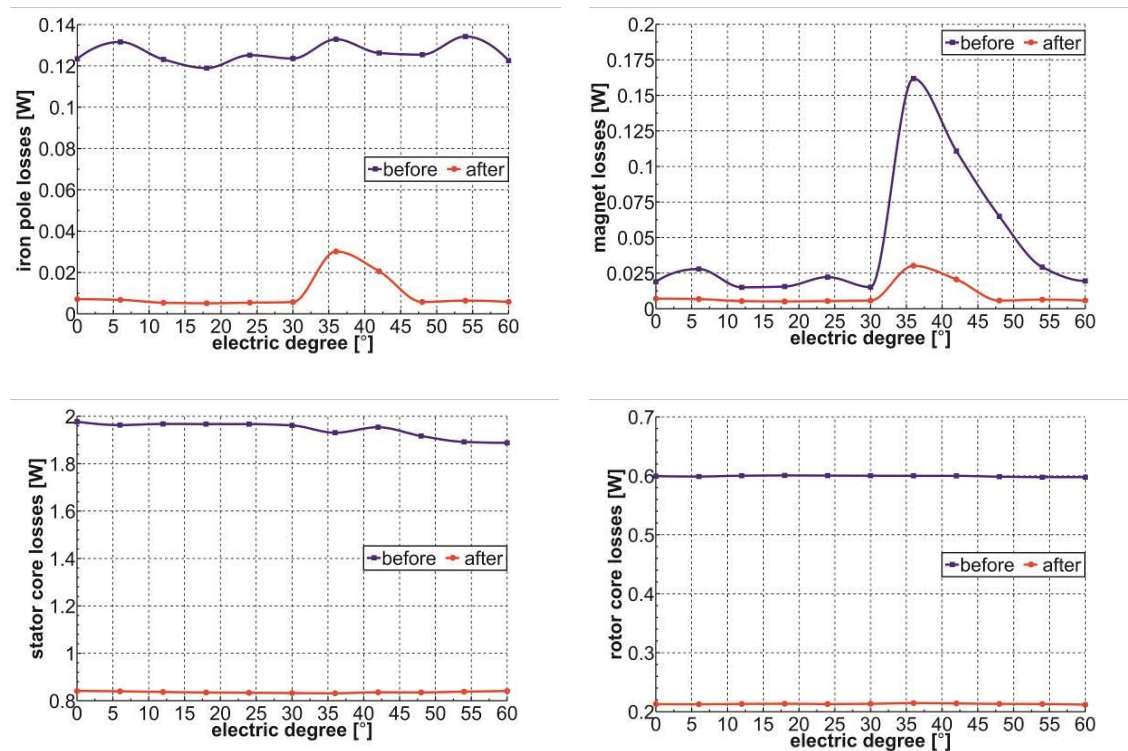


Figure 9. Current density in the rotor part of the 3D FE model: a) initial, b) optimal.

Furthermore, in case of magnet part of rotor the eddy current losses are computed under assumption that has conductive material properties as follows resistivity $1.6e-6 \Omega \cdot m$. Figure 9 shows the distribution of the iron losses and the magnet eddy-current losses calculated in both the initial and optimal models for the first rotor angular position $\vartheta = 0$.



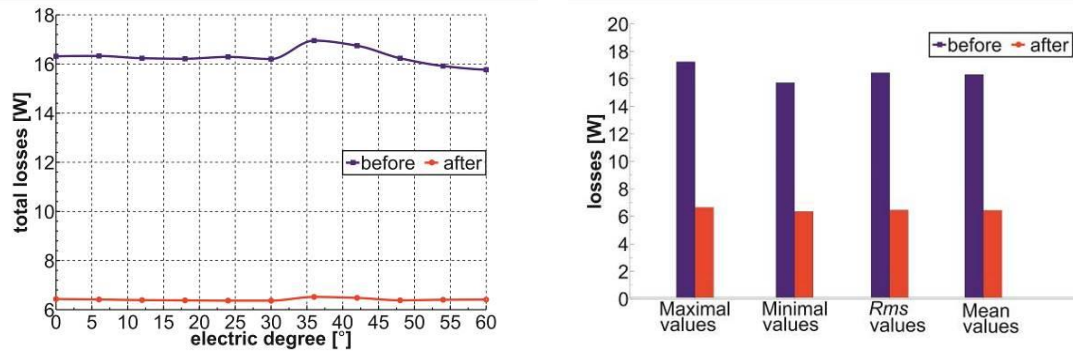


Figure 10. Distribution of losses in the particular parts of the ECPSM versus electrical degree at 1000 rpm.

The distribution of eddy current losses calculated in a particular part of the 3D model of the ECPSM is presented on Figure 10. It can be noticed that for the optimized structure, the mean of total losses has decreased 60%, while the mean of iron pole losses and magnet losses have fallen approximately 92% and 80%, respectively. Finally, some essential results of the optimization obtained from the 3D analysis are summarized in Table 3.

Table 3. Values of some physical parameters of the ECPSM before and after optimization

Considered quantities	Before optimization	After optimization	Ratio
Cogging Torque [Nm]			
Rectified mean values [Nm]	0.71	0.07	90.78%↓
RMS values [Nm]	0.83	0.08	89.89%↓
Minimal values [Nm]	-1.32	-0.07	94.41%↓
Maximal values[Nm]	1.30	0.21	83.60%↓
3D Eddy Currents Losses [W]			
Mean of iron pole losses [W]	0.13	0.01	91.79%↓
Mean of magnet losses [W]	0.05	0.01	79.79%↓
Mean of stator core losses [W]	1.95	0.84	56.79%↓
Mean of rotor core losses [W]	0.60	0.21	64.47%↓
Mean of total losses [W]	16.32	6.44	60.52%↓
Other quantities			
Torque Ripple [Nm]	1.09	0.70	35.54%↓
THD of the back-EMF [V/V]	0.17	0.06	62.90%↓
Rectified mean values of the back-EMF [V]:	222.20	179.94	19.02%↓
Mean of flux density \mathbf{B}_r in the air-gap [T]	0.19	0.16	16.48%↓
RMS of torque [Nm]	2.08	1.71	17.84%↓
Mass of iron pole [g]	16.50	13.70	17.00%↓
Mass of PM pole [g]	16.50	11.72	29.00%↓
Mass of six units of tooth base [g]	6.0	4.0	25.00%↓

7. Conclusions

In this work, the shape of the iron and the PM rotor pole as well as tooth base of the stator have been simultaneously investigated in order to minimize the level of noise and vibration in the ECPSM machine that can be used in modern drives for electro-mobiles. Such an approach has been undertaken as the main target of this paper to design the unique PM machine with the minimum of both the cogging torque and the torque ripple. The developed 2/3D models confirm, that the application of topological and shape sensitivity via the multi-level set method with the AVM and the TV regularization leads to a significant reduction of both the CT and the TR according to the assumed level of the back-EMF. The simulation results obtained for the optimized machine configuration are depicted in Figure 8, whereas the distribution of the eddy current losses in both the iron and magnet parts of the machine under consideration is depicted in Figure 10. It is worth mentioning that the mean value of total losses has been reduced about 60,5% for the whole optimized structure. Furthermore, the mass of the machine has been also reduced around 17% for the PM pole, 29% for the iron pole and 25% for the tooth base in stator. The main result for the optimization was summarized in Table 3. This work also highlights the unique design challenges of the proposed methodology.

Acknowledgements

The project nanoCOPS (Nanoelectronic COupled Problems Solutions) is supported by the European Union in the FP7-ICT-2013-11 Program under the grant agreement number 619166, the SIMUROM project is supported by the German Federal Ministry of Education and Research (05M13PXB). The author would also like to thank Dr. Piotr Paplicki for his help and Professor Ryszard Pałka for the opportunity to use the ECPS machine model in our research.

References

- Allaire, G., Jouve, F., Gournay F. and Toader A.M. (2004), "Structural optimization using topological and shape sensitivity via a level set method", Internal Report 555, Ecole Polytechnique, pp. 1-21.
- Amstutz, S., Takahashi, T. and Vexler, B. (2007), "Topological sensitivity analysis for time-dependent problems", *ESAIM: Control, Optimisation and Calculus of Variations*, Vol. 14 No.3, pp. 427-455.
- Bertotti, G. (1988), "General properties of power losses in soft ferromagnetic materials", *IEEE Trans. on Magn.*, Vol. 24, No. 1, pp. 621-630.
- Bianchi, N. and Bolognani, S. (2002), "Design techniques for reducing the cogging torque in surface-mounted PM motors", *IEEE Trans. Ind. Appl.*, Vol. 38, No. 5, pp. 1259-1265.
- Borghetti C.A., Casadei D., Cristofolini A., Fabri M., Serra G. (1999), Application of a Multiobjective minimization technique for reducing the Torque Ripple in Permanent-Magnet motors, *IEEE Trans. on Magnet.*, Vol. 35, No. 5, pp. 4238-4246.
- Braess, H. and Wriggers P. (2000), "Arbitrary Lagrangian Eulerian finite element analysis of free surface flows", *Computer Methods in Applied Mechanics and Engineering*, Vol. 190, No. 1/2, pp. 95-109.
- Burger, M., Hackl, B. and Ring, W. (2004), "Incorporating Topological Derivatives into Level Set Methods", *J. Comp. Phys.*, Vol.194 no. 1, pp. 344-362.
- Cea, J., Garreau, S., Guillaume, P., and Masmoudi, M. (2000), "The shape and topological optimizations connection", *Computer Methods in Applied Mechanics and Engineering*, Vol. 118, pp. 713-726.
- Chan, T.F., Tai, X.-C. (2004), "Level set and total variation regularization for elliptic inverse problems with discontinuous coefficients", *J. of Comput. Physics*, Vol. 193, No.1, pp. 40-66.
- Chen, S., Namuduri, C., and Mir, S. (2002), "Controller-induced parasitic torque ripples in a PM synchronous motor", *IEEE Trans. Ind. Appl.*, Vol. 38 No.5, pp.1273-1281.

- Cimrák, I., Melicher, V. (2007), "Sensitivity analysis framework for micromagnetism with application to optimal shape design of magnetic random access memories", *Inverse Problems*, Vol. 23 No. 2, pp. 563-588.
- Conway J. (1997), *A Course in Functional Analysis*, Springer, New York, NY.
- Di Barba, P.M. (2010), *Multi-objective shape design in electricity and magnetism*, Springer.
- Di Barba, P., Mognaschi, M.E., Pałka, R., Paplicki, P., Szkolny, S. (2012), "Design optimization of a permanent-magnet excited synchronous machine for electrical automobiles", *JAEM*, Vol. 39 No. 1/4, pp. 889-895.
- Durand, S., Cimrák, I. and Sergeant, P. (2009) "Adjoint variable method for time-harmonic Maxwell equations", *COMPEL*, Vol. 28 No. 5, pp. 1203-1215.
- Dyck, D.N., Lowther, D.A. (1994), "A method of computing the sensitivity of electromagnetic quantities to changes in material and sources", *IEEE Trans. on Magn.* Vol. 30 No.5, pp. 3415-3418.
- Favre, E., Cardoletti, L. and Jufer, M. (1993), "Permanent-magnet synchronous motors: A comprehensive approach to cogging torque suppression", *IEEE Trans. Ind. Appl.*, Vol. 29 No. 6, pp. 1141-1149.
- Gawrylczyk, K.M., Putek, P. (2008), "Multi-frequency sensitivity analysis of 3D models utilizing impedance boundary condition with scalar magnetic potential", *Advanced Computer Techniques in Applied Electromagnetics*, IOS Press, Vol. 30, pp. 64-71.
- Gieras F., Wing M. (2008), *Permanent magnet motor technology*, John Wiley & Sons Ltd.
- Hawe, G., Sykulski, J. (2008), "Scalarizing cost-effective multi-objective optimization algorithm made possible with kriging", *COMPEL*, Vol. 27 No. 4, pp. 836-844.
- Haug, E., Choi, K., Komkov, V. (1986), *Design Sensitivity Analysis of Structural Systems*, Academic Press.
- He, L., Kao Ch. Y., Osher S. (2007), "Incorporating topological derivatives into shape derivatives based level set methods", *J. of Comput. Physics*, Vol. 225 No.1, pp. 891-909.
- Hughes A. (2006), *Electric Motors and Drives*, Elsevier Ltd.
- Husain I. (2005), *Electric and hybrid vehicles. Design Fundamentals*, CRC Press.
- Igarashi, I. and Watanabe, K. (2010), "Complex Adjoint Variable Method for Finite-Element Analysis of Eddy Current Problems", *IEEE Trans. on Magn.*, Vol. 46 No. 8, pp. 1154-1156.
- Jahns, T.M. and Soong, W. L. (1996), "Pulsating torque minimization techniques for permanent magnet AC motor drives –A review", *IEEE Trans. Ind. Electron.*, Vol. 43 No.2, pp. 321-330.
- Kim, D., Ship, K., and Sykulski, J. (2004), "Applying Continuum Design Sensitivity Analysis combined with standard EM software to shape optimization in magnetostatic problems", *IEEE Trans. and Magn.*, Vol. 40 No. 6, pp. 1156-1159.
- Kim, D., Sykulski, J., and Lowther, D. (2009), "The implications of the use of composite materials in electromagnetic device topology and shape optimization", *IEEE Trans. on Magn.*, Vol. 45 No. 2, pp. 1154-1156.
- Kim, Y.S. and Park, I.H. (2010), "Topology optimization of rotor in synchronous reluctance motor using level set method and shape design sensitivity", *IEEE Trans. on Appl. Supercond.*, Vol. 20 No. 3, pp. 1093-1096.
- Lee, J.H., Kim, D.H., and Park, I.H. (2003), "Minimization of Higher Back-EMF Harmonics in Permanent Magnet motor using shape design sensitivity with B-Spline parameterization", *IEEE Trans. on Magnet.* Vol. 39 No. 3, pp. 1269-1272.
- Li, T. and Slemon, G. (1988), "Reduction of cogging torque in permanent magnet motors", *IEEE Trans. Magn.*, Vol. 24 No. 6, pp. 2901-2903.
- Li, M., Lowther, D.A. (2011), "Topological sensitivity analysis for steady state eddy current problems", *IEEE Trans. on Magn.*, Vol. 47 No. 5, pp. 1294-1297.
- Lim, S., Min, S., and Hong, J. P. (2012), "Low torque ripple rotor design of the interior permanent magnet motor using the multi-phase level-set and phase-field concept", *IEEE Trans. on Magn.*, Vol. 48 No. 2, pp. 907-909.
- Makini, Z., Besbes, M., and Marchand, C. (2007), "Multiphysics design methodology of permanent-magnet synchronous motors", *IEEE Trans. on Magn.*, Vol. 56 No. 4, pp. 1524-1530.
- Maler, T. (2009), *A Study of Multi-Objective Optimization Methods: for Engineering Applications*, VDM Verlag.
- Masmoudi, M., Pommier, J., and Samet B. (2005), "The topological asymptotic expansion for the Maxwell equations and some application", *Inverse Problem*, Vol. 21 No. 2, pp.547-564.
- May, H., Pałka, R., Paplicki, P., Szkolny, S., Canders, W.R. (2011), "New concept of permanent magnet excited synchronous machines with improved high-speed features", *Archives of Electrical Engineering*, Vol. 60 No. 4, pp. 531-540.

- May, H., Pałka, R., Paplicki, P., Szkolny, S., Wardach, M. (2012), "Comparative research of different structures of a permanent-magnet excited synchronous machine for electric vehicles", *Electrical Review*, R. 88 No. 12a, pp. 53-55.
- Nakata, T., Takahashi, N., Fujiwara, K. and Ahagon, A. (1988), "Periodic boundary condition for 3-D magnetic field analysis and its applications to electrical machines", *IEEE Trans. on Magn.*, Vol. 24 No. 6, pp. 2694-2696.
- Osher, S.J., Sethian, J.A. (1988), "Fronts propagating with curvature dependent speed: algorithms based on Hamilton-Jacobi formulations", *J. Comput. Phys.*, Vol. 79 No. 1, pp.12-49.
- Osher, S.J., Santosa, F. (2001), "Level set methods for optimization problems involving geometry and constraints I. Frequencies of a two-density inhomogeneous drum", *J. of Comput. Physics*, Vol. 171 No. 1, pp. 272-288.
- Pałka, R., Paplicki, P., Wardach, M. (2013), "Design and Analysis of an Electrically Controlled Permanent Magnet Excited Synchronous Machine", COMPUMAG 2013 – 19 International Conference on the Computation of Electromagnetic Fields, 2013, Budapest, Hungary.
- Paplicki, P. (2010), "The new generation of electrical machines applied in hybrid drive car", *Electrical Review*, R. 86 No. 6, pp. 101-103.
- Paplicki, P. (2014), "Design optimization of the electrically controlled permanent magnet excited synchronous machine to improve flux control range", *Electronica ir elektrotechnica*, accepted for the publication.
- Park, H., Shin, H. (2003), "Shape identification for natural convection problems using the adjoint variable method", *J. of Comput. Physics*, Vol. 186 No.1, pp. 198-211.
- Park I.H., Lee H.B, Kwak I.G. and Hahn S.Y.(1994), Design Sensitivity Analysis for Steady State Eddy Current Problems by Continuum Approach, *IEEE Trans. on Magn.*, Vol. 30, No. 5, pp. 3411–3414.
- Putek, P., Paplicki, P., Slodička, M. and Pałka, R. (2012), "Minimization of cogging torque in permanent magnet machines using the topological gradient and adjoint sensitivity in multi-objective design", *JAEM*, Vol. 39 Nos 1/4, pp. 933–940.
- Putek, P., Paplicki, P., and Pałka, R. (2014a), Low Cogging Torque Design of Permanent Magnet Machine Using Modified Multi-Level Set Method With Total Variation Regularization, *IEEE Trans. on Magn.*, Vol. 50 No. 2, pp. 657–660.
- Putek P., Paplicki P., and Pałka R. (2014b), "Topology optimization of rotor poles in a permanent-magnet machine using level set method and continuum design sensitivity analysis", *COMPEL*, Vol. 66 No. 3, pp.711-728.
- Schumacher, A., Kobolev, V., Eschenauer, H. (1996), "Bubble method for topology and shape optimization of structures", *J. Struct. Optimi.*, Vol.8 No. 1, pp. 42-51.
- Sethian, J.A. (1999), *Level set methods and fast marching methods: evolving interfaces in computational geometry, fluid mechanics, computer vision, and material science*, Cambridge University Press.
- Sokołowski, J., Żochowski, A. (1999), "Topological derivatives for elliptic problems", *Inverse Problems*, Vol. 15 No. 1, pp.123-124.
- Sokołowski, J., and Zolesio, J.P. (1992), *Introduction to Shape Optimization. Shape Sensitivity Analysis*, Springer-Verlag Berlin Heilderberg.
- Srinath, S., Mittal, D.N. (2010), "An adjoint method for shape optimization in unsteady viscous flows", *J. of Comput. Physics*, Vol. 229 No. 6, pp. 1994-2008.
- Vese, L. A. and Chan, T. F. (2002), "A multiphase level set framework for image segmentation using the Mumford and Shah model", *Int. J. Comput. Vis.*, Vol. 50 No. 3, pp. 271-293.
- Vogel, C. R., Omam, M. E. (1998), "Fast, robust total variation-based reconstruction of noisy, blurred images", *IEEE Trans. on Image Processing*, Vol.7 No. 6, pp. 813-824.
- Yamada, T., Izui, K., Nishiwaki, S. and Takezawa, A. (1010), "A topology optimization method based on the level set method incorporating a fictitious interface energy," *Comput. Methods Appl. Mech. Eng.*, Vol. 199 No. 45/48, pp. 2876-2891.
- Zhu, Z. Q. and Howe, D. (2000), "Influence of design parameters on cogging torque in permanent magnet machines", *IEEE Trans. Energy Convers.*, Vol. 15 No. 4, pp. 407-412.
- Ziemer, W.P. (1989), *Weakly differentiable functions. Sobolev Spaces and Functions of Bounded Variation*. Series: Graduate Texts in Mathematics, Vol. 120 Springer-Verlang, New York.

